Int. J. Electrochem. Sci., 17 **(2022)** Article Number: 221063, doi: 10.20964/2022.10.63

International Journal of
ELECTROCHEMICAL
SCIENCE
www.electrochemsci.org

Synthesis of TiO_2/graphene Oxide Nanocomposite and its Application for Visible Light Assisted Photocatalytic Degradation of Crystal Violet Dye

Yuan Xu[1,2], *Yunsheng Qian*[1,*], *Jianliang Qiao*[2], *Jun Niu*[2], *Shaobo Cui*[2], *Shengzhao Wang*[2]

[1] School of Electronic and Optical Engineering, Nanjing University of Science & Technology, Nanjing, 210094, China
[2] School of Information Engineering, Nanyang Institute of Technology, Nanyang, 473004, China
[*]E-mail: qian_science@sina.com

Received: 29 December 2021 / *Accepted:* 27 January 2022 / *Published:* 10 September 2022

The photocatalysts based on the nanocomposite of TiO_2 and x% graphene oxide (TiO_2/GO-x) (x = 1, 3, 5, 8 and 10) have been successfully synthesized by a solvethermal method. The nanocomposites were characterized using XRD, SEM, EIS, UV-Visible spectroscopy and photocatalytic analyses. The XRD and SEM analyses indicated that the nanosheets of GO were completely incorporated by TiO_2 NPs in the solvethermal process. Results of EIS analysis demonstrated a lower resistance for carrier transfer between the TiO_2/GO modified electrode and the electrolyte. Study on the optical properties of the samples using UV-Visible spectroscopy revealed that the optical band gaps of TiO_2, TiO_2/GO-1, TiO_2/GO-3, TiO_2/GO-5, TiO_2/GO-8 and TiO_2/GO-10 were obtained as 3.27, 3.15, 3.10, 3.05, 3.03 and 2.98 eV, respectively, indicating the narrowing of the band gap with increased GO content in nanocomposite. The photocatalytic results for degradation of 100 mg/l crystal violet **(**CV) dye aqueous solution containing 5 mg of photocatalysts showed that the high degradation rate and complete removal of dye were achieved in the presence of TiO_2/GO-8 photocatalyst after 90 and 80 minutes of irradiation of UV and visible light, respectively, indicating the optimum content of GO in TiO_2/GO based-photocatalyts under both of UV and visible light irradiations was evaluated 8%. Comparison between the photocatalytic degradation performance of TiO_2/GO-8 nanocomposite and the other reported literature for treatment CV dye illustrated that the TiO_2/GO-8 nanocomposite had effective performance for degradation of CV dye because of the large specific surface area, high adsorption capacity and high photocatalytic activity under UV and visible light irradiations.

Keywords: Photodegradation; Crystal violet dye, Photocatalyst; TiO_2/GO nanocomposites

1. INTRODUCTION

Hexamethyl pararosaniline chloride[cyclohexa-2,5-dien-1-ylidene]-dimethylazanium chloride] Crystal violet, also known as gentian violet, is a triarylmethane dye that is widely used in the textile

and paper industries for the preparation of paints and dyes [1, 2]. It is also used for staining cell nuclei in histological studies [3, 4]. The antibacterial agent, antiseptic, antifungal, anthelmintic, and antflatulent properties of CV lead to application in dentistry and medicine such as treatment of fungal infections, thrush, impetigo, yeast infections and burn wounds [5-7].

However, studies showed that CV should be regarded as a biohazard substance because of its clastogenic characterization that it promotes tumor and cancer cells in some species of fish [8, 9]. Moreover, it may be harmful when it inhaled or ingested because it causes irritation when exposed to skin and eyes [10, 11]. Accordingly, the use of CV dye in cosmetic products is limited in some European countries [12]. This product has been withdrawn from the Canadian market due to safety problems. As a result of their hazardous effects on health and the environment, CV dyes must be removed from industrial wastewater before it is discharged [13-15].

Many research studies have been focused on the decolonization of CV solution from contaminated water by foam separation [16], electrocoagulation [17], Fenton process [18], chemical oxidation and microfiltration [19, 20], sono-sorption [21], and photodegradation based on photocatalytic reactions [22-25]. Among these treatment methods, photodegradation is conducted under the joint action of light and the semiconductor-based photocatalysts [26]. It is a low cost, high efficiency and an environmental protection method [27-29]. A large number of semiconductor-based photocatalysts have been fabricated using TiO_2 and ZnO because of their high chemical stability, low cost, biologically benign and environmentally friendly nature [30-32].

However, the photocatalytic activity of TiO_2 is also limited by some crucial restrictive factors such as the rapid recombination of the photogenerated electron-hole pairs and poor affinity toward organic pollutants in wastewaters treatment [33-35]. Thus, several studies have been conducted on band gap engineering of nanostructured photocatalysts to enhancement the absorption ability and degradation sufficiency of organic pollutants [36-38]. Narrowing down the TiO_2 band gap can promote the quantum efficiency and the solar energy conversion efficiency [39-41]. Therefore, this study presented synthesis the TiO_2/GO nanocomposites, and structural and photocatalytic studies for degradation of crystal violet dye.

2. EXPERIMENTAL

2.1. TiO_2/GO *nanocomposites preparation*

The solvethermal method was applied to synthesize TiO_2/GO nanocomposites [42]. 60 mg of GO (diameter of 1-5 μm, Globalchemical Factory Co., Ltd., China) was ultrasonically dispersed in 50 ml of isopropyl alcohol (99%, Merck, Germany) for 120 minutes. Subsequently, tetrabutyl titanate (97%, Sigma-Aldrich) was added to the dispersed mixture of GO and the mixture was stirred for 20 minutes. Next, 1 ml of deionized (DI) water was added drop by drop and the resultant mixture was transferred into the oven and heated at 170°C for 20 minutes. Then, the product was rinsed, filtered, and dispersed in DI water before being dried at 85°C overnight. The quality ratio of GO in TiO_2: GO was prepared as 1%, 3%, 5%, 8% and 10%, which were marked as TiO_2/GO-x (x = 1, 3, 5, 8 and 10).

2.2. Characterization

XRD analysis was carried out by an X-ray diffractometer (XRD; Miniflex600, $CuK_{\alpha 1}$ radiation λ = 0.154056 nm, Rigaku Corp., Tokyo, Japan), and the morphology of the nanostructures was observed by field-emission scanning electron microscopy (FESEM; JEOL JSM 6300F, Tokyo, Japan) and transmission electron microscope (TEM; JEM-ARM200F, JEOL, Japan). The optical properties of samples were analyzed by the UV–vis spectrometer (HITACHI, U-3900H, Tokyo, Japan). For electrochemical impedance spectroscopy (EIS) analysis, the prepared nanostructures were used for modification of the glassy carbon electrode (GCE) surface. The GCE was carefully polished with 0.05 μm alumina slurry (99%, Henan Union Precision Material Co., Ltd., China) onto the microcloth, and sonicated successively with a mixture of DI water and ethanol for 5 minutes to obtain a mirror-like surface. Afterwards, 5mg/ml of TiO_2/GO and TiO_2 suspensions were separately dispersed in mixture of DMF/Nafion and dropped on the GCE surface. Then, the TiO_2/GO/GCE and TiO_2/GCE were dirtied under infrared light. The EIS measurements were conducted on an electrochemical workstation (Autolab, PGSTAT302N, Herisau, Switzerland) with a three-electrode system, including the modified GCE as working electrode, Ag/AgCl as reference electrode and Pt foil as the auxiliary electrode. EIS experiments were performed in frequency range from 10^{-1} Hz to 10^5 Hz with an amplitude of 5 mV peak-to-peak using ac signals in electrolyte solution of 0.5 M Na_2SO_4.

2.3. Photocatalytic degradation study

For photocatalytic degradation studies, UV-C lamp (6 W, maximum emission peak at 365 nm, Philips, India) and visible LEDs (7W, λ = 405 nm) were used as UV and visible light source in the reactor, respectively. 100 ml of 100 mg/l CV dye aqueous solution containing 5mg of catalyst was irradiated perpendicularly with light sources. The distance between the light source and the reactor was 1 cm. The measurements were carried out at room temperature. Before the degradation measurements, the mixture of dye aqueous solution and catalyst was stirred in the dark for 30 minutes to reach the adsorption-desorption equilibrium between the dye molecules and the catalyst surface. Degradation of dyes was analyzed by recording variations of the absorption band maximum using a UV spectrophotometer (UV-3600, Shimadzu, Japan) and degradation efficiency was determined using according equation (1) [36, 37, 43]:

$$\text{Degradation efficiency (\%)} = \frac{C_0 - C_t}{C_0} \times 100 = \frac{I_0 - I_t}{I_0} \times 100 \qquad (1)$$

Where, C_0 and C denote the initial and variable concentrations of dye, respectively. I_0 and I also are the initial and variable absorbance, respectively.

To study the phototalyst performance in a real sample, the real sample of textile wastewater was centrifuged at 1000 rpm and the supernatant was used for the preparation of the 5mg/l CV solution. The prepared 5 mg/l CV solution with deionized water was used as a control sample.

3. RESULTS AND DISCUSSION

3.1. Morphology and crystallinity analyses

Powder XRD patterns for the GO, TiO_2 and TiO_2/GO-8 nanocomposites are displayed in Figure 1. As seen in XRD patterns of GO, the characteristic plane of (001) of the graphitic structure is observed at 11.12° [44]. In TiO_2 and TiO_2/GO-8 nanocomposites, the reflections at 2θ = 25.21°, 37.76°, 47.75°, 54.25°, 62.15°, 69.29° and 74.79° are observed to have characteristic plans of (101), (004), (200), (105), (213), (116), and (215), respectively, associated with the anatase phase of TiO_2 (JCPDS card No. 00-021-1272). There is the additional peak of the (001) plane of GO for TiO_2/GO-8 nanocomposites, corresponding that in the solvethermal process, the sheets of GO were completely incorporated by TiO_2 NPs.

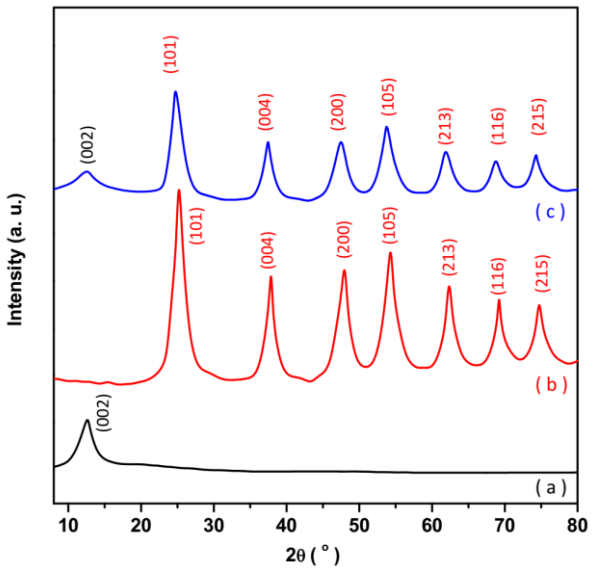

Figure 1. Powder XRD diffractograms of (a) GO, (b) TiO_2, and (c) TiO_2/GO-8.

The SEM images of GO, TiO_2 and TiO_2/GO-8 nanocomposites are shown in Figure 2. The SEM image of GO in Figure 2a depicts the wrinkled and folded morphology of nanosheets. The TiO_2/GO-8 nanocomposites morphology in Figure 2c shows that TiO_2 NPs have been distributed uniformly over the GO nanosheets. During the solvethermal process, the sufficient oxygen functionalities on the GO nanosheets cause interactions with the cations and create anchoring sites for the nucleation and growth of TiO_2 NPs, indicating the growth of TiO_2/GO nanocomposites [45]. The higher porosity, more exposed new edges provide a larger specific surface area and more active photocatalytic sites [46-48].

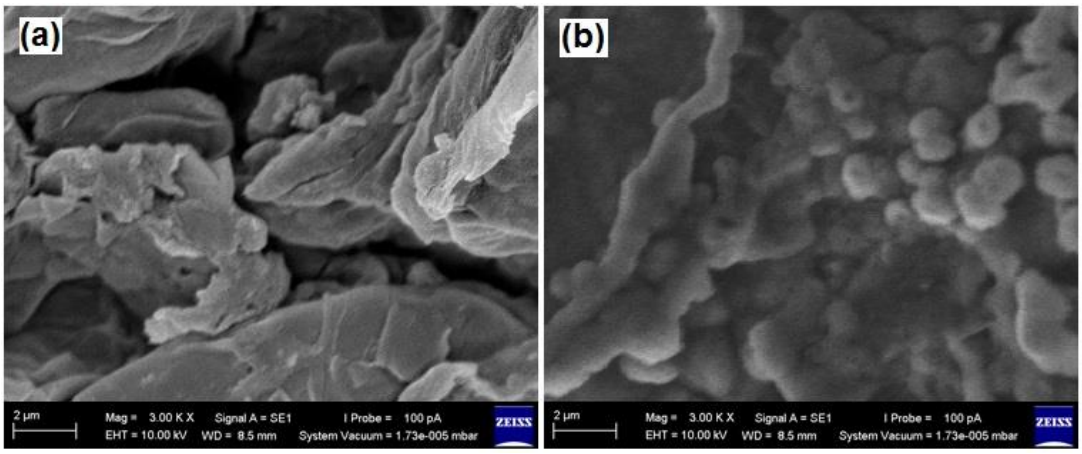

Figure 2. The SEM images of (a) GO, (b) TiO_2/GO-8 nanocomposites.

3.2. Electrochemical impedance studies

EIS measurements were used to study the electrochemical characteristics and interface properties of modified electrodes. The obtained Nyquist plots from Figure 3 show the semicircle at higher frequencies where the diameter of the semicircle is signified by charge-transfer resistance. As observed, the charge-transfer resistance value for TiO_2/GO-8/GCE is smaller than that for TiO_2/GCE, and TiO_2/GCE is smaller than bare GCE, indicting lower resistance for carrier transfer between TiO_2/GO-8/GCE and electrolyte. It demonstrates that GO nanosheets, due to their high electron mobility and -electron conjugation, act as a good electron transporting bridge and can facilitate electron transport in photocatalytic reactions [49-51]. Therefore, on the basis of the above results, it is clear that TiO_2/GO-8 nanocomposite is a highly efficient photocatalyst.

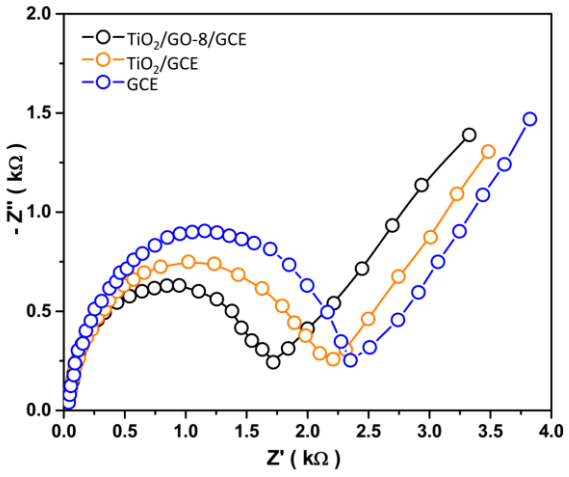

Figure 3. Nyquist plots of TiO_2/GO-8/GCE, TiO_2/GCE and GCE in 0.5 M Na_2SO_4 electrolyte solution.

3.3. Optical analyses

In Figure 4a, the results of the UV-visible spectroscopy analysis of TiO_2 and TiO_2/GO nanocomposites are displayed. As observed, the incorporation of different amounts of GO has an effect on the optical absorption spectra of TiO_2/GO nanocomposites. The UV-visible spectra of the TiO_2 and TiO_2/GO nanocomposites demonstrate similar adsorption profiles. Furthermore, as GO concentration is increased, UV-visible absorption intensity increases with increasing GO content in the nanocomposites, and absorption edges of nanocomposites are red-shifted to higher wavelengths, corresponding to the narrowing of the optical band gap of TiO_2/GO nanocomposites [52-54]. Optical band gap values of TiO_2 and TiO_2/GO nanocomposites are calculated using the Tauc plot according to the following equation [38]:

$$(\alpha h\upsilon)^{1/2} = C(h\upsilon - E) \quad (2)$$

Where α, h, υ, C and E signify the absorption coefficient, Planck's constant (4.1357×10^{-15} eVs), the frequency of light and the proportionality constant, respectively. E and $h\upsilon$ donate the optical band gap of the samples and the photon energy, respectively. Figure 4b exhibits the variation of $(\alpha h\upsilon)^{1/2}$ in term of incident photon energy. The optical band gap value of the samples is ascertained by extrapolating the linear portion of the plot on the X-axis. The point of intersection of the extrapolated straight line on the X-axis determines the amounts of the optical band gap of TiO_2, TiO_2/GO-1, TiO_2/GO-3, TiO_2/GO-5, TiO_2/GO-8 and TiO_2/GO-10 as 3.27, 3.15, 3.10, 3.05, 3.03 and 2.98 eV, respectively, as expected with increasing GO content the red shift in the absorption edge and the decreasing value of the optical band gap. It suggests that the introduction of GO with the abundance of oxygen-containing groups (hydroxyl, epoxy, and carboxyl) can narrow the band gap of nanocomposite, which is associated with the formation of C-Ti bonds and Ti-O-C structures that can effectively shift the valence band and reduce the band gap [55, 56]. Moreover, the band gap narrowing of nanocomposites can broaden the light response into the visible light area [39].

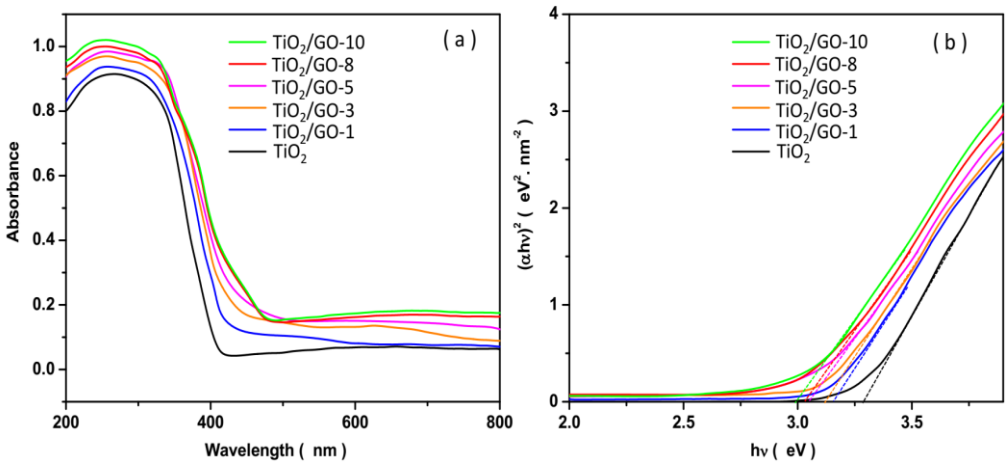

Figure 4. (a) UV-Visible spectra and (b) Tauc plots of TiO_2 and TiO_2/GO nanocomposites

3.3. Photocatalytic degradation studies

The photocatalytic activity of TiO_2 and TiO_2/GO nanocomposites was investigated through the degradation of the CV dye under UV and visible light irradiations and results are shown in Figure 5. Before irradiation with UV light, the samples were kept in darkness for 30 minutes, and after 30 minutes the samples were irradiated under UV and visible light irradiations. Results show that the degradation efficiency in darkness is less than 1.5% and after light irradiation the degradation efficiency is significantly increased, indicating the light effect on dye treatment. Figure 5a depicts the degradation efficiency of the 100 mg/l dye in a blank (without photocatalyt) and in the presence of TiO_2 based-photocatalyts under UV radiation. As observed, the degradation efficiency of blank sample is very inappreciable and it is outstandingly enhanced in the presence of TiO_2 based-photocatalyts. TiO_2, TiO_2/GO-1, TiO_2/GO-3, TiO_2/GO-5, TiO_2/GO-8, and TiO_2/GO-10 degradation efficiency values after 120 minutes are 55.7, 65.2, 81.2, 91.8, 100, and 100%, respectively. The complete degradation of 100 mg/l CV dye is achieved in the presence of TiO_2/GO-8 nanocomposite after 90 minutes of UV irradiation. A comparison between the degradation efficiency values of samples reveals that the presence of the GO in nanocomposite content increases the degradation rate of CV dye. It is suggested that modification or hybridization of TiO_2 based-photocatalyts with GO nanosheets can form the Schottky barrier at the interface between the GO and TiO_2 [57, 58]. This Schottky barrier can remarkably decrease the recombination of the photogenerated electron-hole pairs. In TiO_2/GO nanocomposites, electrons flow from TiO_2 to GO through an interface, which is mainly related to the higher Fermi level of TiO_2 (4.89 eV) than that of GO (∼2.2 eV) [59, 60]. Under UV light irradiation, GO plays a role as an electron acceptor and gains excess photoinduced electrons from TiO_2 while TiO_2 has positive charges, which significantly enhances the efficiency of carriers' separation, and forms a space charge layer and Schottky barrier at the interface between the GO and TiO_2 [45, 61]. This Schottky barrier can act as an electron sink to trap the photoinduced electrons and remarkably decrease the recombination rate of the photogenerated electron-hole pairs [62]. The mechanism of photodegradation of CV using TiO_2/GO nanocomposites may involve the following reactions [30]:

$$TiO_2/GO + hv \rightarrow TiO_2/GO\ (e^- + h^+) \quad (3)$$

$$TiO_2/GO\ (h^+) + H_2O \rightarrow TiO_2/GO\ (^{\bullet}OH) + H^+ \quad (4)$$

$$TiO_2/GO\ (h^+) + OH^- \rightarrow TiO_2/GO\ (^{\bullet}OH) + H^+ \quad (5)$$

$$TiO_2/GO\ (^{\bullet}OH) + H_2O \rightarrow H_2O_2 + H^+ \quad (6)$$

$$TiO_2/GO\ (e^-) + O_2 \rightarrow TiO_2/GO\ (O_2^{-\bullet}) \quad (7)$$

$$(h^+) \text{ or } O_2^{-\bullet} + CV \rightarrow \text{Intermediate product} \rightarrow \text{Degraded products} \quad (8)$$

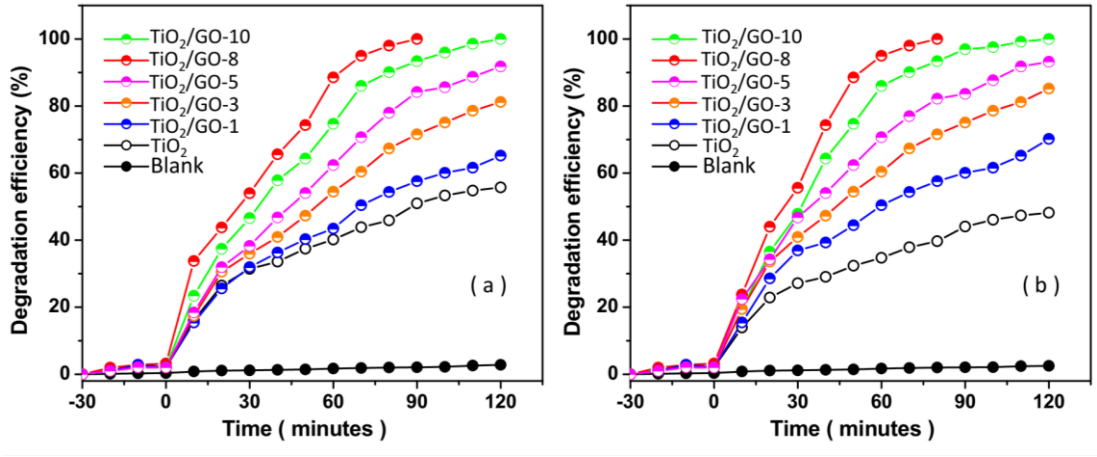

Figure 5. Degradation efficiency of the 100 ml of 100 mg/l CV dye aqueous solution in blank (without photocatalyt) and in presence of 5 mg TiO_2 based-photocatalyts under (a) UV and (b) visible light irradiations.

Figure 5b shows that after 120 minutes of visible light irradiation, the degradation efficiency values of TiO_2, TiO_2/GO-1, TiO_2/GO-3, TiO_2/GO-5, TiO_2/GO-8 and TiO_2/GO-10 reach 48.1, 70.3, 85.2, 93.2, 100 and 100%, respectively. As seen, the degradation efficiency of dye using TiO_2 is decreased and promoted under visible light irradiation toward the UV light irradiation, which is related to its large band gap and great photocatalytic activity under irradiation of UV light. The 100% degradation of 100 mg/l of CV dye is obtained in the presence TiO_2/GO-8 nanocomposite after 80 minutes of visible irradiation. The degradation efficiency of dye using TiO_2/GO nanocomposites is remarkably promoted under visible light irradiation toward the UV light irradiation which attributed to narrowing of band gap and improvement of the visible photocatalytic activity of TiO_2/GO nanocomposites. Furthermore, as observed from the both of Figures 5a and 5b, the degradation rate is increased with an increase the GO content up to 8%, and it is decrease for more addition of GO content in nanocomposite structure. It can be related to light absorption and scattering role of excess GO nanosheets in TiO_2 based-photocatalyts [63], and excessive GO in nanocomposites may act as the electron–hole recombination center and increase the opportunity to more photoindused electrons and holes [64-66]. Therefore, the optimum content of GO in TiO_2/GO nanocomposites for preparation the TiO_2 based-photocatalyts under both of UV and visible light irradiations is 8%.

Table 1 reveals the comparison between the photocatalytic degradation performance of the proposed nanocomposite and the other reported literature for the treatment of CV dye. The results illustrated that the TiO_2/GO-8 nanocomposite has effective performance for degradation of CV dye because of the low cost, simple synthesis method, large specific surface area, high adsorption capacity, and high photocatalytic activity under UV and visible light irradiations [67].

Table 1. Comparison between the photocatalytic degradation performance of proposed nanocomposite and the other reported literature for treatment CV dye

Photocatalyst	**Dye content (mg/l)**	**Light source**	**Degradation time (minute)**	**Degradation efficiency (%)**	**Ref.**
TiO_2/GO-8	100	visible	80	100	This work
		UV	90	100	
TiO_2 nanospheres	50	UV	360	99	[22]
g-C_3N_4/Ag_3VO_4	20	UV	150	34	[23]
Mn doped Polyvinylpyrrolidone-ZnO NPs	10	UV	180	100	[24]
Thioglycerol capped ZnS NPs	10	UV–Visible	180	96	[25]
MWCNTs/Cd-ZnO NPs	10	UV	30	100	[31]
GO capped Ag2S	10	UV	90	99.58	[68]
CeO_2 NPs	1	UV	180	97	[69]
W-doped $Ga_2Zr_2O_7$	10	UV	300	100	[70]
TiO_2 P25	---	UV	60	81	[30]
NiO nanospheres	---	UV	60	98	[30]

The applicability of the developed photocatalyst was investigated for degradation of CV in a prepared real sample of textile wastewater. The degradation of 5 mg/l CV prepared in deionized water and prepared in real samples of textile wastewater was investigated using TiO_2/GO-8 under irradiation of visible light. As observed from Figure 6, the 100% degradation of CV solution prepared in deionized water and prepared in real samples of textile wastewater is obtained after 50 and 58 minutes, respectively. Therefore, the degradation time for the sample prepared with a real sample of textile wastewater sample is higher than the sample prepared with deionized water, which is associated with presence of other organic compounds and dye molecules in wastewater.

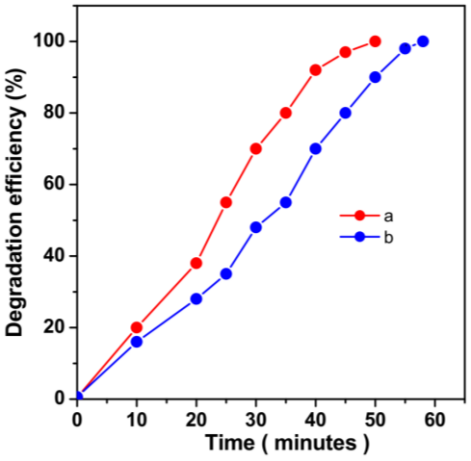

Figure 6. The degradation of 5 mg/l CV (a) prepared in deionized water and (b) prepared in real samples of textile wastewater were investigated using TiO_2/GO-8 under irradiation of visible light.

4. CONCLUSION

In summary, the photocatalysts based on TiO_2/GO-x nanocomposites with x% GO (x = 1, 3, 5, 8 and 10) have been successfully synthesized by a solvethermal method. The nanocomposites were characterized using XRD, SEM and EIS analyses. The analysis results indicated that in the solvethermal process the sheets of GO were completely incorporated by TiO_2 NPs. Results of EIS measurements demonstrated lower resistance for carrier transfer between the TiO_2/GO modified electrode and electrolyte. UV-Visible spectroscopy analysis of TiO_2 and TiO_2/GO_x nanocomposites revealed that the optical band gap of TiO_2, TiO_2/GO-1, TiO_2/GO-3, TiO_2/GO-5, TiO_2/GO-8 and TiO_2/GO-10 as 3.27, 3.15, 3.10, 3.05, 3.03 and 2.98 eV, respectively, as expected with increasing GO content, the red shift in the absorption edge and the decreasing value of the optical band gap and the narrowing of the band gap of nanocomposite. The photocatalytic results for the degradation of 100 ml of 100 mg/l CV dye aqueous solution containing 5 mg of photocatalysts showed that the complete degradation of 100 mg/l CV dye was achieved in the presence of TiO_2/GO-8 photocatalyst after 90 and 80 minutes of irradiation of UV and visible lights, respectively. The optimum content of GO in TiO_2/GO nanocomposites for the preparation of the TiO_2 based-photocatalyts under both of UV and visible light irradiations was evaluated at 8%. The degradation efficiency of dye using TiO_2/GO nanocomposites was remarkably promoted under visible light irradiation toward UV light irradiation irradiation, which was attributed to the narrowing of band gap and improvement of the visible photocatalytic activity of TiO_2/GO nanocomposites. A comparison between the photocatalytic degradation performance of TiO_2/GO-8 nanocomposite and the other reported literature for the degradation of CV dye illustrated that the TiO_2/GO-8 nanocomposite had effective performance for degradation of CV dye because of the low cost, simple synthesis method, large specific surface area, high adsorption capacity, and high photocatalytic activity under UV and visible light irradiations.

ACKNOWLEDGEMENT
This work was sponsored in part by the Science and Technology project of Henan Province (212102210217); Key scientific research project of higher education of Education Department Henan Province (21A140019).

References

1. Y. Fu, H. Chen, R. Guo, Y. Huang and M.R. Toroghinejad, *Journal of Alloys and Compounds*, 888 (2021) 161507.
2. X. Zhang, Y. Tang, F. Zhang and C.S. Lee, *Advanced Energy Materials*, 6 (2016) 1502588.
3. H. Maleh, M. Alizadeh, F. Karimi, M. Baghayeri, L. Fu, J. Rouhi, C. Karaman, O. Karaman and R. Boukherroub, *Chemosphere*, (2021) 132928.
4. S.-S. Yang, X.-L. Yu, M.-Q. Ding, L. He, G.-L. Cao, L. Zhao, Y. Tao, J.-W. Pang, S.-W. Bai and J. Ding, *Water Research*, 189 (2021) 116576.
5. E. Ozkan, E. Allan and I.P. Parkin, *ACS omega*, 3 (2018) 3190.
6. C.-X. Chen, S.-S. Yang, J. Ding, G.-Y. Wang, L. Zhong, S.-Y. Zhao, Y.-N. Zang, J.-Q. Jiang, L. Ding and Y. Zhao, *Applied Catalysis B: Environmental*, 298 (2021) 120495.

7. M. Khosravi, *Journal of Eating Disorders*, 8 (2020) 1.
8. S. Mani and R.N. Bharagava, *Reviews of Environmental Contamination and Toxicology Volume 237*, (2016) 71.
9. L. He, C. Yang, J. Ding, M.-Y. Lu, C.-X. Chen, G.-Y. Wang, J.-Q. Jiang, L. Ding, G.-S. Liu and N.-Q. Ren, *Applied Catalysis B: Environmental*, 303 (2022) 120880.
10. Y. Orooji, B. Tanhaei, A. Ayati, S.H. Tabrizi, M. Alizadeh, F.F. Bamoharram, F. Karimi, S. Salmanpour, J. Rouhi and S. Afshar, *Chemosphere*, 281 (2021) 130795.
11. G. Li, S. Huang, N. Zhu, H. Yuan, D. Ge and Y. Wei, *Chemical Engineering Journal*, 421 (2021) 127852.
12. H. Li, J. Tang, Y. Kang, H. Zhao, D. Fang, X. Fang, R. Chen and Z. Wei, *Applied Physics Letters*, 113 (2018) 233104.
13. X. Chen, D. Wang, T. Wang, Z. Yang, X. Zou, P. Wang, W. Luo, Q. Li, L. Liao and W. Hu, *ACS applied materials & interfaces*, 11 (2019) 33188.
14. D. Xu and H. Ma, *Journal of Cleaner Production*, 313 (2021) 127758.
15. A. Medghalchi, M. Akbari, Y. Alizadeh and R.S. Moghadam, *Journal of current ophthalmology*, 30 (2018) 353.
16. X.-l. Zhang, Z.-l. Wu, H.-j. Zheng and H.-m. Ding, *The Chinese Journal of Process Engineering*, 6 (2008) 015.
17. D. Ghosh, C. Medhi, H. Solanki and M. Purkait, *Journal of environmental protection science*, 2 (2008) 25.
18. H. Zhang, H. Gao, C. Cai, C. Zhang and L. Chen, *Water science and technology*, 68 (2013) 2515.
19. Y. Zhang, J. Ren, Q. Wang, S. Wang, S. Li and H. Li, *Biochemical Engineering Journal*, 168 (2021) 107930.
20. S. Jana, M. Purkait and K. Mohanty, *Applied clay science*, 50 (2010) 337.
21. S.M. Yakout, M.R. Hassan, A.A. Abdeltawab and M.I. Aly, *Journal of Cleaner Production*, 234 (2019) 124.
22. V. Jadhav, R. Dhabbe, S. Sabale, G. Nikam and B. Tamhankar, *Universal Journal of Environmental Research & Technology*, 3 (2013) 667.
23. S. Wang, D. Li, C. Sun, S. Yang, Y. Guan and H. He, *Applied Catalysis B: Environmental*, 144 (2014) 885.
24. M. Mittal, M. Sharma and O. Pandey, *Journal of nanoscience and nanotechnology*, 14 (2014) 2725.
25. M. Sharma, T. Jain, S. Singh and O. Pandey, *Solar Energy*, 86 (2012) 626.
26. W.-F. Lai and W.-T. Wong, *Asian Journal of Pharmaceutical Sciences*, 16 (2021) 577.
27. Q. Dai, K. Shen, W. Deng, Y. Cai, J. Yan, J. Wu, L. Guo, R. Liu, X. Wang and W. Zhan, *Environmental Science & Technology*, 55 (2021) 4007.
28. H. Liu, X. Li, Z. Ma, M. Sun, M. Li, Z. Zhang, L. Zhang, Z. Tang, Y. Yao and B. Huang, *Nano Letters*, 21 (2021) 10284.
29. M. Khosravi, *Open Access Macedonian Journal of Medical Sciences*, 8 (2020) 553.
30. R. Vahini, P.S. Kumar and S. Karuthapandian, *Applied Physics A*, 122 (2016) 744.
31. M.F. Sanakousar, V. C.C, Victor M. Jiménez-Pérez, B.K. Jayanna, Mounesh, A.H. Shridhar and K. Prakash, *Journal of Hazardous Materials Advances*, 2 (2021) 100004.
32. M. Hu, Y. Wang, Z. Yan, G. Zhao, Y. Zhao, L. Xia, B. Cheng, Y. Di and X. Zhuang, *Journal of Materials Chemistry A*, 9 (2021) 14093.
33. D. Chen, Y. Cheng, N. Zhou, P. Chen, Y. Wang, K. Li, S. Huo, P. Cheng, P. Peng and R. Zhang, *Journal of Cleaner Production*, 268 (2020) 121725.
34. H. Fu, B. Gao, C. Hu, Z. Liu, L. Hu, J. Kan, Z. Feng and P. Xing, *Nanotechnology*, 33 (2021) 075703.
35. R. Wang, H. Xie, X. Lai, J.-B. Liu, J. Li and G. Qiu, *Molecular Catalysis*, 515 (2021) 111881.

36. B. Gong, P. Wu, J. Yang, X. Peng, H. Deng and G. Yin, *International Journal of Electrochemical Science*, 16 (2021) 21023.
37. Z. Zhang, Y. Yang and D. Cheng, *International Journal of Electrochemical Science*, 16 (2021) 21115.
38. J. Zhu and Z. Jiang, *International Journal of Electrochemical Science*, 16 (2021) 210318.
39. J. Li, C.-H. Liu, X. Li, Z.-Q. Wang, Y.-C. Shao, S.-D. Wang, X.-L. Sun, W.-F. Pong, J.-H. Guo and T.-K. Sham, *Chemistry of Materials*, 28 (2016) 4467.
40. G. Li, S. Huang, N. Zhu, H. Yuan and D. Ge, *Journal of Hazardous Materials*, 403 (2021) 123981.
41. R. Rezapour-Nasrabad, *Electronic Journal of General Medicine*, 15 (2018) em73.
42. Y. Huang, D. Chen, X. Hu, Y. Qian and D. Li, *Nanomaterials*, 8 (2018) 431.
43. S. Ameen, M.S. Akhtar, M. Nazim and H.-S. Shin, *Materials letters*, 96 (2013) 228.
44. R. Savari, J. Rouhi, O. Fakhar, S. Kakooei, D. Pourzadeh, O. Jahanbakhsh and S. Shojaei, *Ceramics International*, 47 (2021) 31927.
45. Y. Ren, Y. Dong, Y. Feng and J. Xu, *Catalysts*, 8 (2018) 590.
46. C.-T. Hsieh, W.-S. Fan, W.-Y. Chen and J.-Y. Lin, *Separation and Purification Technology*, 67 (2009)
47. H. Savaloni, E. Khani, R. Savari, F. Chahshouri and F. Placido, *Applied Physics A*, 127 (2021) 1.
48. H. Savaloni and R. Savari, *Materials Chemistry and Physics*, 214 (2018) 402.
49. L. Sang, L. Lei and C. Burda, *Nano-Micro Letters*, 11 (2019) 97.
50. H.Y. Hafeez, S.K. Lakhera, M. Ashokkumar and B. Neppolian, *Ultrasonics Sonochemistry*, 53 (2019) 1.
51. S.M. Mahmoudinezhad Dezfouli and S. Khosravi, *Indian Journal of Forensic Medicine & Toxicology*, 15 (2021) 2674.
52. K. Ullah, S. Ye, S.-B. Jo, L. Zhu, K.-Y. Cho and W.-C. Oh, *Ultrasonics sonochemistry*, 21 (2014)
53. R. Hassanzadeh, A. Siabi-Garjan, H. Savaloni and R. Savari, *Materials Research Express*, 6 (2019) 106429.
54. S.M.M. Dezfouli and S. Khosravi, *European Journal of Translational Myology*, 30 (2020) 291.
55. Q. Zhang, N. Bao, X. Wang, X. Hu, X. Miao, M. Chaker and D. Ma, *Scientific Reports*, 6 (2016) 38066.
56. W. Gao, M. Wang, C. Ran, X. Yao, H. Yang, J. Liu, D. He and J. Bai, *Nanoscale*, 6 (2014) 5498.
57. M.D. Purkayastha, S. Sil, N. Singh, P.P. Ray, G.K. Darbha, S. Bhattacharyya, A.I. Mallick and T.P. Majumder, *FlatChem*, 22 (2020) 100180.
58. M.A. Delavar and P. Karimian, *Pakistan Journal of Medical & Health Sciences*, 14 (2020) 1686.
59. M.K. Rabchinskii, S.A. Ryzhkov, D.A. Kirilenko, N.V. Ulin, M.V. Baidakova, V.V. Shnitov, S.I. Pavlov, R.G. Chumakov, D.Y. Stolyarova, N.A. Besedina, A.V. Shvidchenko, D.V. Potorochin, F. Roth, D.A. Smirnov, M.V. Gudkov, M. Brzhezinskaya, O.I. Lebedev, V.P. Melnikov and P.N. Brunkov, *Scientific Reports*, 10 (2020) 6902.
60. Q. Yang, M. Hu, J. Guo, Z. Ge and J. Feng, *Journal of Materiomics*, 4 (2018) 402.
61. D. Ge, H. Yuan, J. Xiao and N. Zhu, *Science of The Total Environment*, 679 (2019) 298.
62. A. Meng, L. Zhang, B. Cheng and J. Yu, *Advanced Materials*, 31 (2019) 1807660.
63. S. Khosravi and S.M.M. Dezfouli, *Systematic Reviews in Pharmacy*, 11 (2020) 913.
64. P. Wang, S. Zhan, Y. Xia, S. Ma, Q. Zhou and Y. Li, *Applied Catalysis B: Environmental*, 207 (2017) 335.
65. T. Chen, C. Song, M. Fan, Y. Hong, B. Hu, L. Yu and W. Shi, *International Journal of Hydrogen Energy*, 42 (2017) 12210.

66. C. Shi, Z. Wu, F. Yang and Y. Tang, *Solid State Sciences*, 119 (2021) 106702.
67. B. Ji, F. Zhang, X. Song and Y. Tang, *Advanced materials*, 29 (2017) 1700519.
68. A. Dasari and V. Guttena, *Materials Today Communications*, 19 (2019) 157.
69. P.K. Sharma and O. Pandey, *Journal of Sol-Gel Science and Technology*, (2021) 1.
70. H. Abbas, R.A. Nasr, R. Abu-Zurayk, A. Al Bawab and T.S. Jamil, *Royal Society open science*, 7 (2020) 191632.